


Evaluation of the fission barrier values using the experimental values of the ratio $\Gamma_f(E)/\Gamma_n(E)$

O. I. Davydovska ¹, V. Yu. Denisov ^{1,2} and I. Yu. Sedykh ³

¹*Institute for Nuclear Research, Prospect Nauki 47, 03028 Kiev, Ukraine*

²*Faculty of Physics, Taras Shevchenko National University of Kiev, Prospect Glushkova 2, 03022 Kiev, Ukraine*

³*Financial University under the Government of the Russian Federation, Leningradsky Prospekt 49, 125993 Moscow, Russian Federation*

 (Received 27 July 2021; revised 18 November 2021; accepted 10 January 2022; published 20 January 2022)

The experimental values of the ratio $\Gamma_f(E)/\Gamma_n(E)$ are well described for the nuclei $^{180,181,182,184}\text{W}$, ^{185}Re , $^{186,187,188,190}\text{Os}$, $^{189,191}\text{Ir}$, $^{192,193,194,196}\text{Pt}$, $^{197,195}\text{Au}$, $^{196,198,199,200}\text{Hg}$, ^{201}Tl , $^{207,209}\text{Bi}$, $^{208,210,211,212}\text{Po}$, and ^{213}At . The values of fission barrier height are deduced using a statistical approach for a description of the ratio $\Gamma_f(E)/\Gamma_n(E)$. The dependence of the fission barrier on the thermal excitation energy of the compound nucleus is taken into account in the calculations. The obtained values of 29 fission barrier heights are entirely consistent with the available experimental data as well as with the results of the macroscopic-microscopic finite-range liquid-drop model.

DOI: [10.1103/PhysRevC.105.014620](https://doi.org/10.1103/PhysRevC.105.014620)

I. INTRODUCTION

The ratio $R(E) = \Gamma_f(E)/\Gamma_n(E)$ of the fission width $\Gamma_f(E)$ to the neutron evaporation width $\Gamma_n(E)$ is an important and widely used characteristic of various nuclear reactions related to the decay of strongly excited heavy nuclei [1–9]. This ratio is extracted in various experiments and shows the competition between neutron emission and fission [1–11]. The widths $\Gamma_f(E)$ and $\Gamma_n(E)$ depend on the energy-level density $\rho(e)$, the fission barrier B_f , the neutron separation energy B_n , and the total excitation energy E of the nucleus [1–14].

The fission barrier depends on the temperature T or the thermal excitation energy $\varepsilon = a(\varepsilon)T^2$ of the compound nucleus [7,10,11,14–24]. Here $a(\varepsilon)$ is the energy-level density parameter [25–27]. The fission barrier can be calculated in the framework of the Strutinsky shell correction prescription [28,29]. The value of the fission barrier in the framework of this prescription has both the liquid-drop and the shell-correction contributions. The shell-correction contribution consists of the saddle-point and the ground-state parts. The temperature dependence of the constants of the liquid-drop model is negligible at $T \lesssim 2$ MeV [20,23], therefore the liquid-drop contribution to the fission barrier height B_{ld} depends weakly on the thermal excitation energy in this temperature interval [7,14,18,20,23]. In contrast with this, the shell-correction energies are strongly damped with an increase of ε at $T \lesssim 2$ MeV and approach to zero at $T \gtrsim 2$ MeV [15–17,19]. As a result, the value of the shell-correction contribution to the fission barrier $B_{\text{shell}}(\varepsilon)$ drops strongly with an increase of ε . Therefore, the full fission barrier height $B_f(\varepsilon) \approx B_{\text{ld}} + B_{\text{shell}}(\varepsilon)$ decreases significantly with an increase of ε due to the damping of the shell-correction contribution to the fission barrier at $T \lesssim 2$ MeV [7,10,14–17,19].

The fission width and, as a result, the ratio $R(E)$ should be affected by the dependence of the fission barrier on the

thermal excitation energy of a compound nucleus. A new expression for the fission width, which takes into account the dependence of the fission barrier on ε , has been derived recently [14]. There are the experimental data for the ratio $R(E)$, [1–3,8]. Therefore, it is interesting to deduce the values of the fission barrier using the experimental values of the ratio $\Gamma_f(E)/\Gamma_n(E)$ and compare these values with the experimental data and the values obtained in other approaches.

The same set of the statistical model parameters is used in our approach for the calculation of the fission and neutron emission widths. In contrast with this, different values of the asymptotic level-density parameters for the fission a_0^f and neutron emission a_0^n channels are applied for the fitting of the ratio $\Gamma_f(E)/\Gamma_n(E)$ to the experimental data in Refs. [1–5,8,9]. Moreover, a fission barrier independent of the excitation energy is considered in previous studies of the ratio $\Gamma_f(E)/\Gamma_n(E)$.

We have estimated the fission barrier values in the framework of our approach for three nuclei in our previous paper [7]. Now we extend our consideration to 29 nuclei: $^{180,181,182,184}\text{W}$, ^{185}Re , $^{186,187,188,190}\text{Os}$, $^{189,191}\text{Ir}$, $^{192,193,194,196}\text{Pt}$, $^{197,195}\text{Au}$, $^{196,198,199,200}\text{Hg}$, ^{201}Tl , $^{207,209}\text{Bi}$, $^{208,210,211,212}\text{Po}$, and ^{213}At . The experimental values of the ratio $\Gamma_f(E)/\Gamma_n(E)$ for these 29 nuclei given in Ref. [2] are used for evaluating the fission barrier values in the framework of our approach.

The paper is organized as follows: The expressions for the fission and neutron emission widths are shortly described in Sec. II. Detailed discussions of the results are given in Sec. III. Conclusions are presented in Sec. IV.

II. THE DECAY WIDTHS

Let us consider the fission width $\Gamma_f(E)$ and the neutron evaporation width $\Gamma_n(E)$ in detail.

The total excitation energy E of the compound nucleus at the saddle point may be distributed among the thermal excitation energy of the compound nucleus ε , the potential energy related to the fission barrier $B_f(\varepsilon)$, and the kinetic energy K of the collective coordinates connected to the fission distortion. The fission width is proportional to the number of states available for the fission at the saddle point [12]. Due to this the fission width depends on the total excitation energy E , the fission barrier height $B_f(\varepsilon)$, and the energy level density $\rho(\varepsilon)$.

The fission width of an excited nucleus with the fission barrier dependent on the excitation energy is derived in our recent paper [14]. It is given by

$$\Gamma_f(E) = \frac{2}{2\pi\rho(E)} \int_0^{\varepsilon_{\max}} d\varepsilon \frac{\rho(\varepsilon)}{N_{\text{tot}}} N_{\text{saddle}}(\varepsilon). \quad (1)$$

Here the ratio $\rho(\varepsilon)/N_{\text{tot}}$ is the probability to find the fissioning nucleus with the intrinsic thermal excitation energy ε in the fission transition state,

$$N_{\text{tot}} = \int_0^{\varepsilon_{\max}} d\varepsilon \rho(\varepsilon) \quad (2)$$

is the total number of states available for fission in the case of the energy-dependent fission barrier, and

$$\begin{aligned} N_{\text{saddle}}(\varepsilon) &= \int_0^{E-B_f(\varepsilon)-\varepsilon} dK \rho(E-B_f(\varepsilon)-K) \\ &= \int_{\varepsilon}^{E-B_f(\varepsilon)} d\rho(\varepsilon) \end{aligned} \quad (3)$$

is the number of states available for the fission at the thermal excitation energy ε . ε_{\max} is the maximum value of the intrinsic thermal excitation energy of the compound nucleus at the saddle point, which is determined as the solution of the equation

$$\varepsilon_{\max} + B_f(\varepsilon_{\max}) = E. \quad (4)$$

This equation is related to the energy conservation law, i.e., the sum of thermal ε_{\max} and potential $B_f(\varepsilon_{\max})$ energies at the saddle point equals the total excitation energy E . Note that, in the case of an energy-independent fission barrier, the fission width $\Gamma_f(E)$ is equal to the Bohr-Wheeler width [12], see, for details, Ref. [14]. The Bohr-Wheeler fission width with the energy-independent fission barrier is used for the analysis of $\Gamma_f(E)/\Gamma_n(E)$ in Refs. [1–5,8,9].

The neutron emission width is written in the form [7,30]

$$\begin{aligned} \Gamma_n(E) &= \frac{1}{2\pi\rho(E)} \int_0^{E-B_n} dK \rho_d(E-B_n-K) \\ &= \frac{1}{2\pi\rho(E)} \int_0^{E-B_n} d\varepsilon \rho_d(\varepsilon), \end{aligned} \quad (5)$$

where $\rho_d(\varepsilon)$ is the energy-level density of the daughter nucleus formed after the neutron emission. The advantages of this expression for the neutron width are discussed in detail in Ref. [30]. We consider that the neutron separation energy B_n is independent of ε at $T \lesssim 2$ MeV.

We use the back-shifted Fermi gas model [25,26] for a description of the energy-level density $\rho(\varepsilon)$ in Eqs. (1)–(3)

and (5), which is given by

$$\rho(\varepsilon) = \frac{\pi^{1/2} \exp(2\sqrt{a(\varepsilon-\Delta)(\varepsilon-\Delta)})}{12[a(\varepsilon-\Delta)]^{1/4}(\varepsilon-\Delta)^{5/4}}, \quad (6)$$

where

$$a(\varepsilon) = a_0 \left\{ 1 + \frac{E_{\text{shell}}^{\text{emp}}}{\varepsilon} [1 - \exp(-\gamma\varepsilon)] \right\} \quad (7)$$

is the level-density parameter [26,27],

$$a_0 = 0.0722396A + 0.195267A^{2/3} \text{ MeV}^{-1} \quad (8)$$

is the asymptotic level-density parameter obtained at high excitation energies, when all shell effects are damped [26,27], $E_{\text{shell}}^{\text{emp}}$ is the empirical shell correction value [26,31], $\gamma = 0.410289/A^{1/3} \text{ MeV}^{-1}$ is the damping parameter [26,27], and A is the number of nucleons in the nucleus. According to the prescription of Ref. [26], the value of the empirical shell correction $E_{\text{shell}}^{\text{emp}}$ is calculated as the difference between the experimental value of the nuclear mass and the liquid drop component of the mass formula [26,31]. The back-shift energy is described by the expression $\Delta = 12n/A^{1/2} + 0.173015 \text{ MeV}$ [26], where $n = -1, 0, \text{ and } 1$ for odd-odd, odd- A , and even-even nuclei, respectively. The pairing force dependence of the back-shifted energy-level density is not considered at any energy in Ref. [26].

The energy-level density $\rho(\varepsilon)$ is indefinite at $\varepsilon = \Delta$, see Eq. (6). To avoid this problem, the special parametrization of the energy-level density, which coincides with the Fermi gas formula after a few hundreds of keV, is usually applied; see, for details, Ref. [26]. The values of ε used in the calculation of the ratio $R(E)$ in our consideration are significantly higher than hundreds of keV. Besides this, the leading contributions into the integrals in Eqs. (1)–(3) and (5) are linked to high values of ε due to the exponential dependence of $\rho(\varepsilon)$ on ε . Therefore, we put $\rho(\varepsilon) = 0$ at $\varepsilon \leq \Delta + 0.1 \text{ keV}$.

The values of the asymptotic level-density parameter a_0 , which are applied in our calculation of the fission and neutron emission widths, are determined by Eq. (8). In contrast with this, the values of the asymptotic level-density parameters for fission a_0^f and neutron emission a_0^n channels are different in Refs. [1–5,8,9] because they are used for data fitting. For example, the values of ratio a_0^f/a_0^n for nuclei considered in our work belong to the range from 0.08 to 1.15 in Ref. [2].

According to the Strutinsky shell correction prescription [14–17,19,28,29] the fission barrier is presented as

$$B_f(\varepsilon) = B_{\text{ld}}(\varepsilon) + B_{\text{shell}}(\varepsilon) = B_{\text{ld}}(\varepsilon) + B_{\text{sp}}(\varepsilon) + B_{\text{par}}(\varepsilon), \quad (9)$$

where

$$B_{\text{ld}}(\varepsilon) = E_{\text{ld}}^{\text{saddle}}(\varepsilon) - E_{\text{ld}}^{\text{gs}}(\varepsilon) \quad (10)$$

is the liquid-drop contribution to the fission barrier,

$$B_{\text{sp}}(\varepsilon) = E_{\text{sp}}^{\text{saddle}}(\varepsilon) - E_{\text{sp}}^{\text{gs}}(\varepsilon) \quad (11)$$

is the shell contribution to the fission barrier related to the nonuniform distribution of the single-particle energies around the Fermi level, and

$$B_{\text{par}}(\varepsilon) = E_{\text{par}}^{\text{saddle}}(\varepsilon) - E_{\text{par}}^{\text{gs}}(\varepsilon) \quad (12)$$

is the pairing force contribution to the fission barrier. Here $E_{\text{ld/sp/par}}^{\text{saddle}}$ and $E_{\text{ld/sp/par}}^{\text{gs}}$ are the liquid-drop, single-particle, pairing shell-correction energies of the nucleus at the saddle and ground-state deformations, respectively.

The temperature dependence of the constants of the liquid-drop model is negligible at $T \lesssim 2$ MeV [20,23]. Therefore, the liquid-drop contribution to the fission barrier height B_{ld} depends weakly on the thermal excitation energy $\varepsilon \lesssim \varepsilon_{T=2}$ [7,14,18,20,23], where $\varepsilon_{T=2}$ is the thermal excitation energy of nucleus at $T = 2$ MeV.

The exponential damping of the single-particle shell-correction contribution to the fission barrier $B_{\text{sp}}(\varepsilon)$ with an increase of ε is discussed in Refs. [6,7,10,11,14,21,22]. Now we are using this approximation again.

The pairing correlation is broken at the critical temperature $T_{\text{cr}} = [\varepsilon_{\text{cr}}/a(\varepsilon_{\text{cr}})]^{1/2} \approx 0.5$ MeV [32,33]; therefore, the contribution of the pairing force to the fission barrier equals zero at $\varepsilon \geq \varepsilon_{\text{cr}}$. As noted earlier, the pairing-force contribution to the energy-level density has not been taken into account. For the sake of consistency, we neglect the pairing-force contribution to the fission barrier. Note that the pairing contribution to fission barrier $B_{\text{par}}(\varepsilon)$ is close 1 MeV at $\varepsilon = 0$ and decreases to zero at ε close to ε_{cr} [7,21,22]. The values of the fission barrier in the nuclei considered in our work are greater than 18 MeV (see Table I in the next section), so the contribution of pairing to the fission barrier is an order of magnitude smaller.

As a result, the fission barrier exponentially decreases with the thermal energy ε at $\varepsilon \lesssim \varepsilon_{T=2}$ [6,7,10,11,14,21,22], i.e.,

$$\begin{aligned} B_f(\varepsilon) &= B_{\text{ld}} + B_{\text{sp}} \exp(-\gamma_D \varepsilon) \\ &= B_{\text{ld}} + B_{\text{shell}} \exp(-\gamma_D \varepsilon). \end{aligned} \quad (13)$$

Here $B_{\text{ld}} = B_{\text{ld}}(0)$ and γ_D is the damping coefficient.

Note that the exponential damping of the fission barriers of various superheavy nuclei with increasing ε has been confirmed in the framework of the finite-temperature self-consistent Hartree-Fock + BCS approach with the Skyrme force [21,22]. The calculated values of the inverse barrier damping parameter for various superheavy nuclei lie in the range $10 \text{ MeV} \leq \gamma_D^{-1} \leq 30 \text{ MeV}$ [21]. As a result, the damping of the fission barrier with an increase of ε is significant and depends on the numbers of protons and neutrons in the nucleus [21]. This damping is very important for the calculation of the cross section of superheavy nuclei production in nuclear reactions [10,11]. The same temperature dependence of the fission barrier and the similar variation range of γ_D are applied for lighter nuclei in our approach for $R(E)$ now.

The temperature and thermal energy of the nucleus in the framework of the back-shifted Fermi gas model are determined for $E > \Delta$. Therefore, the dependence of the fission barrier on thermal energy should take into account the back-shifted energy Δ . Due to this, we should replace $B_f(E)$ on $B_f(E - \Delta)$.

The pairing contribution to both the fission barrier and the energy-level density is ignored at values of thermal excitation energy $\varepsilon \geq \varepsilon_{\text{cr}}$. This strongly simplifies the consideration of the width ratio $R(E)$ discussed in our paper. Note that few experimental points of $R(E)$ are measured at energies $\varepsilon \leq \varepsilon_{\text{cr}}$ only and ignored in our consideration.

It may seem that the parameters γ_D in Eq. (13) and γ in Eq. (7) should be the same because these parameters relate to the damping of the shell structure with a rising of the excitation energy of the compound nucleus. However, this is not true. The parameter γ is obtained by fitting the experimental data for the energy-level densities in different nuclei for various excitation energies using the phenomenological dependence of the energy-level density parameter described by Eq. (7) [26,27]. The experimental data for the energy-level densities include the single-particle levels, multiparticle-multihole levels, and other microscopic levels of various nature. The value of γ smoothly reduces with the number of nucleons in nuclei, because $\gamma \propto A^{-1/3}$ [see discussion after Eq. (8)]. The parameter γ_D is found by the fitting of the values of the fission barrier heights calculated in the framework of the finite-temperature self-consistent Hartree-Fock + BCS approach with the Skyrme force at different excitation energies (or temperatures) [21,22]. The values of γ_D are different in various nuclei and irregular on A [21,22]. Thus, the parameter γ_D is related to the damping of the single-particle shell-correction contribution to the fission barrier. In contrast to this, the parameter γ is related to both the single-particle and complex compound-nucleus levels.

III. RESULTS AND DISCUSSION

The values of the ratio $\Gamma_f(E)/[\Gamma_n(E) + \Gamma_f(E)]$ are experimentally studied in $^{180,181,182,184}\text{W}$, ^{185}Re , $^{186,187,188,190}\text{Os}$, $^{189,191}\text{Ir}$, $^{192,193,194,196}\text{Pt}$, $^{197,195}\text{Au}$, $^{196,198,199,200}\text{Hg}$, ^{201}Tl , $^{207,209}\text{Bi}$, $^{208,210,211,212}\text{Po}$, and ^{213}At in the interval of energies E from the one slightly higher than the fission barrier to ≈ 50 MeV [2]. These compound nuclei are formed in (α, f) reactions [2]. We describe the experimental data and obtain the values of the fission barrier of nuclei in the framework of our approach.

The values B_f in these nuclei are two to three times higher than B_n . Therefore, $\Gamma_n(E) \gg \Gamma_f(E)$ and we can write

$$\frac{\Gamma_f(E)}{\Gamma_n(E) + \Gamma_f(E)} \approx \frac{\Gamma_f(E)}{\Gamma_n(E)} \equiv R(E). \quad (14)$$

Due to this, the ratio $R(E)$ will be analyzed below.

The neutron-nucleus potential is formed by the central, centrifugal, and spin-orbit neutron-nucleus potentials. The transmission through the neutron-nucleus potential barrier is important for the emission of the neutron with nonzero angular momentum from the compound nucleus. However, the s -wave neutrons do not have a barrier. The transmission effect for neutron emission with the nonzero orbital momentum is negligible in the study of the ratio $R(E)$ in the set of nuclei considered because the excitation energies of these nuclei in studies of the ratio $R(E)$ are high, i.e., $E > B_f$ and $E > B_n$. As a result, the transmission through the neutron-nucleus potential barrier is not taken into account in the evaluation of $\Gamma_n(E)$ and $R(E)$.

The comparison of the theoretical values of the ratio $R(E)$ calculated using Eqs. (1)–(8), (13), and (14) with the experimental data for $^{180,181,182,184}\text{W}$, ^{185}Re , $^{186,187,188,190}\text{Os}$, $^{189,191}\text{Ir}$, $^{192,193,194,196}\text{Pt}$, $^{197,195}\text{Au}$, $^{196,198,199,200}\text{Hg}$, ^{201}Tl , $^{207,209}\text{Bi}$, $^{208,210,211,212}\text{Po}$, and ^{213}At is presented in Fig. 1. The

TABLE I. The values of parameters used in the calculation of the ratio $R(E)$ for nuclei. B_{ld} and $B_{\text{sp}}(0)$ are the liquid-drop and single-particle shell contributions to the total fission barrier. γ_D^{-1} is the exponential damping of the fission barrier parameter. B_{ld}^{S} is the liquid-drop fission barrier obtained in Ref. [34]. $E_{\text{shell}}^{\text{MNMS}}$ is the shell correction in the ground state of the nucleus obtained in Ref. [35]. $E_{\text{shell}}^{\text{emp}}$ and $E_{\text{shell,d}}^{\text{emp}}$ are the empirical shell correction values [26,31], which are used for the evaluation of $\Gamma_f(E)$ and $\Gamma_n(E)$, respectively. B_n is the neutron separation energy. $B_f(0)$ is the values of the total fission barrier at $\varepsilon = 0$. $B_f^{\text{expt,d,i,j,s,v}}$ are the experimental values of the total fission barrier taken from Refs. [36], [2], [8], [37], and [1], correspondingly. The values of theoretical fission barrier heights B_f^{th} calculated in the macroscopic-microscopic finite-range liquid-drop model [38] are also presented. The values of B_{ld} , B_{ld}^{S} , $B_{\text{sp}}(0)$, $E_{\text{shell}}^{\text{MNMS}}$, $E_{\text{shell}}^{\text{emp}}$, $E_{\text{shell,d}}^{\text{emp}}$, B_n , $B_f(0)$, B_f^{expt} , and B_f^{th} are given in MeV, while the values of γ_D^{-1} are given in MeV^{-1} .

Nucl.	B_{ld}	B_{ld}^{S}	$B_{\text{sp}}(0)$	γ_D^{-1}	$E_{\text{shell}}^{\text{MNMS}}$	$E_{\text{shell}}^{\text{emp}}$	$E_{\text{shell,d}}^{\text{emp}}$	B_n	$B_f(0)$	$B_f^{\text{expt,d}}$	$B_f^{\text{expt,i}}$	$B_f^{\text{expt,j}}$	$B_f^{\text{expt,s}}$	$B_f^{\text{expt,v}}$	B_f^{th}
^{180}W	21.73	20.68	5.57	25.05	-4.31	1.71	1.89	8.41	27.30	23.9	23.9			28.7 ± 3.5	24.57
^{181}W	21.95	20.90	5.72	24.83	-4.80	1.46	1.71	6.67	27.67	23.7	23.7				25.13
^{182}W	22.03	21.10	5.81	25.71	-4.79	1.25	1.46	8.08	27.84	27.1	24.2				25.26
^{184}W	22.53	21.48	5.17	27.04	-5.74	1.25	1.13	7.41	27.70	24.9	24.9				25.44
^{185}Re	20.00	20.07	6.66	30.00	-5.45	1.12	1.00	7.67	26.66	24.0 ± 1.0	24.0				23.66
^{186}Os	19.70	18.65	4.89	30.00	-4.92	1.03	1.25	8.27	24.59	23.4 ± 1.0	22.1			25.8 ± 3.5	21.44
^{187}Os	19.87	18.84	5.19	28.26	-5.31	1.00	1.03	6.29	25.06	22.7 ± 1.0	22.2				21.67
^{188}Os	20.08	19.03	5.02	30.00	-5.22	0.72	1.00	7.99	25.10	24.2 ± 1.0	22.1				21.75
^{190}Os	20.41	19.36	5.75	30.00	-5.71	0.32	0.74	7.79	26.16	23.3	23.3				22.89
^{189}Ir	18.68	17.63	3.91	30.00	-4.53	0.89	1.10	8.18	22.59	22.4 ± 2.5	19.7			21.7 ± 2.5	20.15
^{191}Ir	19.04	17.99	6.00	16.72	-5.32	0.31	0.71	8.03	25.04	23.6 ± 2.5	20.6			22.8 ± 2.5	20.94
^{192}Pt	17.66	16.61	4.45	22.26	-4.31	-0.20	0.59	8.66	22.11	19.2	19.2				20.08
^{193}Pt	17.83	16.78	5.93	21.14	-4.93	-0.33	-0.20	6.26	23.76	20.0	20.0				20.84
^{194}Pt	17.95	16.95	5.65	21.69	-5.43	-1.14	-0.33	8.35	23.60	20.1	20.1				21.47
^{196}Pt	18.29	17.24	6.32	30.00	-6.63	-2.13	-1.44	7.92	24.61	22.5	22.5				23.01
^{195}Au	14.63	15.60	7.13	30.00	-5.55	-1.46	-0.83	8.43	21.76	18.6	18.6				20.54
^{197}Au	16.96	15.91	5.93	30.00	-6.94	-2.64	-2.04	8.07	22.89	20.6	20.6				22.31
^{196}Hg	15.01	14.27	6.36	14.19	-5.82	-2.15	-1.30	8.88	21.37	18.7	18.7		16.9		19.65
^{198}Hg	14.66	14.60	8.14	17.41	-7.20	-3.40	-2.63	8.49	22.80	19.5	19.5		16.6	21.8 ± 1.5	21.45
^{199}Hg	15.80	14.75	7.58	19.13	-8.09	-4.07	-3.40	6.66	23.38	20.2	20.2		18.2		22.24
^{200}Hg	15.94	14.89	7.55	20.82	-8.56	-4.70	-4.07	8.03	23.49	21.2	21.2		17.7		23.23
^{201}Tl	14.63	13.61	8.57	14.42	-8.86	-4.90	-4.33	8.21	23.20	22.3 ± 0.5	19.5		23.1	22.5 ± 1.5	22.23

TABLE I. (Continued.)

Nucl.	B_{ld}	B_{ld}^S	$B_{sp}(0)$	γ_D^{-1}	E_{shell}^{MNMS}	E_{shell}^{emp}	$E_{shell,d}^{emp}$	B_n	$B_f(0)$	$B_f^{expt,d}$	$B_f^{expt,i}$	$B_f^{expt,j}$	$B_f^{expt,s}$	$B_f^{expt,v}$	B_f^{th}
^{207}Bi	12.20	11.70	10.41	16.47	-11.59	-7.17	-6.57	8.10	22.61	23.5	19.9		22.8	21.2 ± 1.5	22.28
										19.9					
^{209}Bi	12.74	11.94	10.94	16.08	-12.83	-8.51	-8.25	7.46	23.68	23.3	21.9		24.3	22.6 ± 1.5	23.88
										21.9					
^{208}Po	11.12	10.54	9.76	12.95	-10.51	-6.07	-5.40	8.40	20.88	24.5	17.9		19.9		20.81
										17.9					
^{210}Po	11.83	10.79	11.51	11.07	-11.79	-7.23	-7.0	7.7	23.34	18.6 ± 2.0	18.2	23.91 ± 0.02	21.2	20.4 ± 1.5	22.14
										20.4 ± 0.5					
										20.5 ± 1.0					
										19.1 ± 0.8					
										19.2 ± 0.8					
										18.2					
^{211}Po	11.90	10.90	8.78	13.58	-10.74	-6.02	-7.23	4.55	20.68	19.7 ± 1.0	17.2	21.49 ± 0.02	20.6		21.33
										17.2					
										20.5					
										21.36 ± 0.01					
^{212}Po	11.97	11.0	7.88	13.73	-9.74	-4.9	-6.0	6.0	19.85	18.6 ± 0.5	16.3	21.97 ± 0.01	19.6	18.6 ± 1.5	20.27
										19.5 ± 1.0					
										16.3					
										22.11 ± 0.02					
^{213}At	10.88	9.90	8.06	10.15	-8.44	-3.67	-5.00	6.02	18.94	15.8 ± 2.0	14.3		17.3	16.8 ± 1.5	18.56
										16.8 ± 0.5					
										17.0 ± 1.0					
										14.3					
										17.2					

experimental values of the ratio $R(E)$ are taken by the digitizing data for (α, f) reactions in the figures of Ref. [2]. The experimental data are well described in Fig. 1. We have taken into account the experimental points with thermal excitation energy $\varepsilon \geq \varepsilon_{cr}$ to avoid any influence of the pairing force.

The values of the liquid-drop contribution to the fission barrier B_{ld} , the single-particle shell contribution to the fission barrier $B_{sp}(0)$, and the barrier damping parameter γ_D^{-1} are obtained by fitting the experimental data for $R(E)$. The values of these parameters used in the calculation of the ratio $R(E)$ for the considered nuclei are presented in Table I.

The values of the empirical shell correction value for the back-shifted Fermi gas model for the energy-level density for the fissioning nuclei E_{shell}^{emp} and the daughter nuclei formed after neutron emission $E_{shell,d}^{emp}$ are picked up from Ref. [31], as recommended in Ref. [26]. The other parameters of the back-shifted Fermi gas model are described in Eq. (6) and in the text after this equation. The value of neutron separation energy B_n is evaluated using the atomic mass table [39]. The values of the energy-level density parameters [26] and the empirical shell correction values [31] are taken without any modifications.

The values of the total fission barrier $B_f(0)$ are obtained using the description of the experimental values of the ratio $R(E)$ in the framework of our approach. The values of $B_f(0)$ are close to the experimental values of the fission barrier B_f^{expt} from Refs. [1,2,8,36,37], see Table I and Fig. 2. Note that the experimental fission barrier values obtained using various reactions leading to the same compound nucleus and various

theoretical approaches are different. Due to this, the values presented in Refs. [2,8,36] for (α, f) reactions are only given in Table I and Fig. 2.

The fission barrier depends on the excitation energy in our approach, see Eq. (12). In contrast with this, a fission barrier independent of the excitation energy is used in the analysis of the experimental data in Refs. [1–3,5,9,36]. Therefore, the differences between the fission barrier values evaluated in different approaches, see Table I and Fig. 2, are reasonable. We present the dependence of fission barriers obtained in different approaches on Z^2/A in Fig. 2.

The values of the fission barrier $B_f(0)$ obtained in our study agree with those found experimentally [1,2,8,36,37], see Table I and Fig. 2. The values of the ^{212}Po and ^{213}At fission barriers calculated in Refs. [5] and [9] are, respectively, 17–18.5, 20.27 and 15.5–18, 18.56 MeV. These values are close to those given in Table I. Note that we use Eq. (8) for the calculation of the asymptotic level-density parameters for fission a_0^f and neutron emission a_0^n channels. In contrast to this, the value of the ratio a_0^f/a_0^n is used for fitting $R(E)$ in various other approaches [1–5,8,9].

Our values of the fission barrier $B_f(0)$ for nuclei with $A \gtrsim 200$ are very close to the theoretical fission barrier heights B_f^{th} calculated in the macroscopic-microscopic finite-range liquid-drop model [38], see Table I and Fig. 2. In lighter nuclei, our values of $B_f(0)$ are larger B_f^{th} on ≈ 1 –2 MeV or $\approx 5\%$ –10%.

The theoretical value of the liquid-drop fission barrier depends on the parameter values of the liquid-drop model and the parametrization of the nuclear fission shapes. The

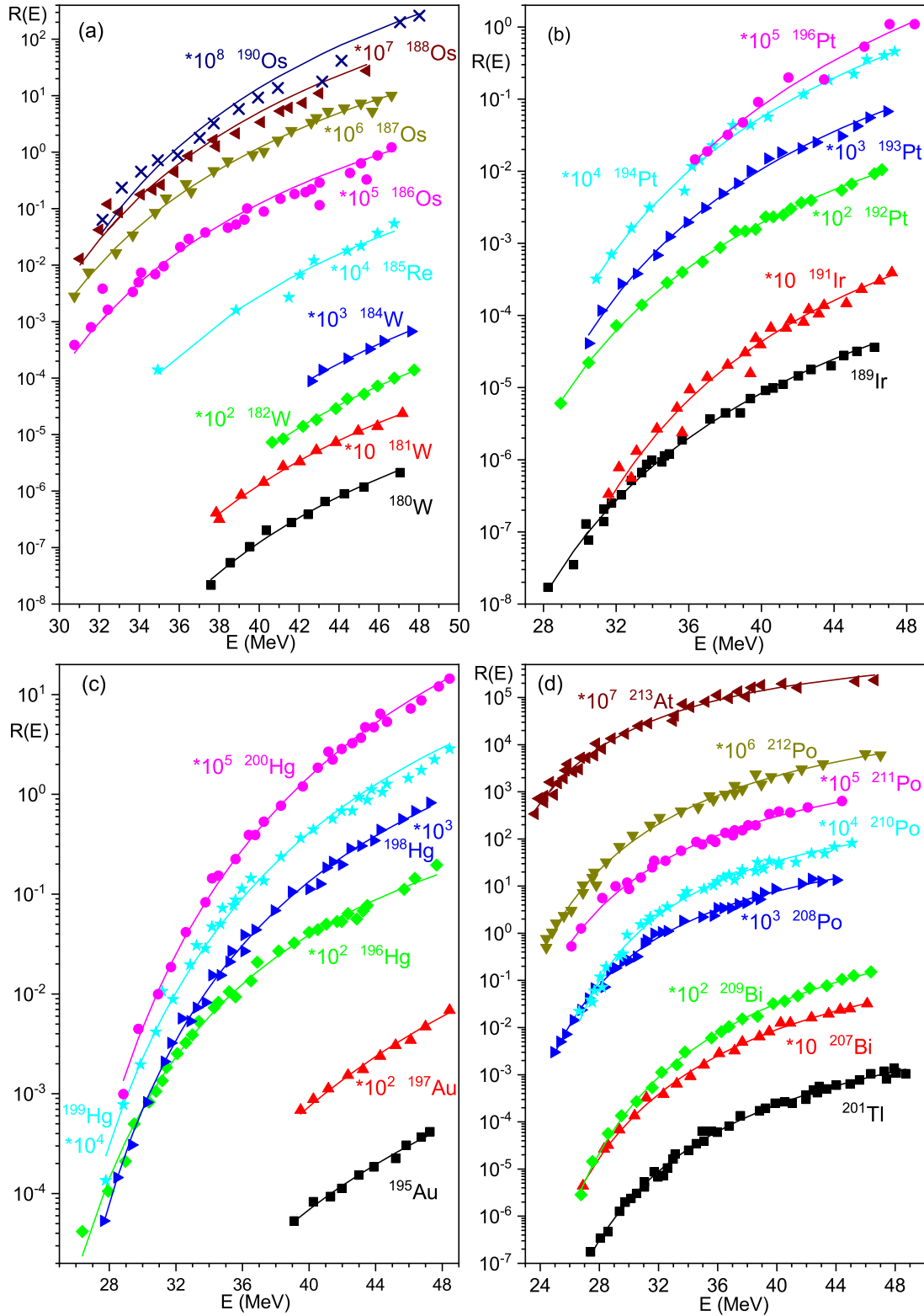


FIG. 1. The energy dependence of the ratios $R(E)$ for (a) $^{180,181,182,184}\text{W}$, ^{185}Re , $^{186,187,188,190}\text{Os}$, (b) $^{189,191}\text{Ir}$, $^{192,193,194,196}\text{Pt}$, (c) $^{197,195}\text{Au}$, $^{196,198,199,200}\text{Hg}$, (d) ^{201}Tl , $^{207,209}\text{Bi}$, $^{208,210,211,212}\text{Po}$, and ^{213}At . The experimental data (dots) are taken from Ref. [2]. The results of our theoretical calculations are shown by solid lines.

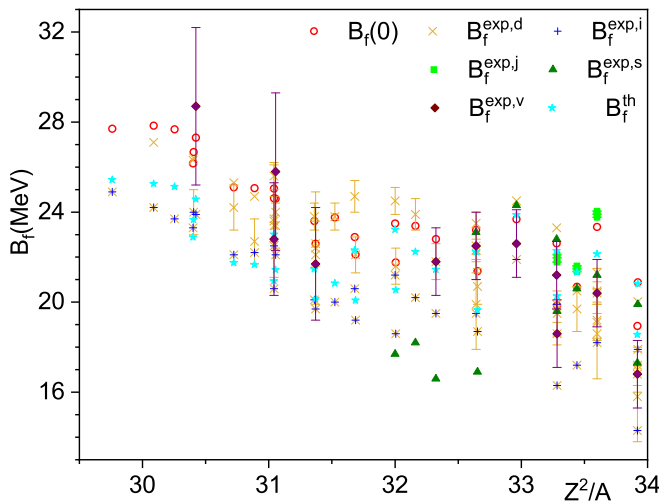


FIG. 2. The dependence of fission barriers B_f obtained in different approaches on Z^2/A . Here $B_f(0)$ are the barrier values evaluated in our approach. The values of $B_f^{\text{exp},d}$, $B_f^{\text{exp},i}$, $B_f^{\text{exp},j}$, $B_f^{\text{exp},s}$, $B_f^{\text{exp},v}$, and B_f^{th} are taken from Refs. [36], [2], [8], [37], [1], and [38], respectively.

values of the liquid-drop fission barrier B_{ld} obtained by fitting the ratio $R(E)$ are larger than the one B_{ld}^{S} calculated in the framework of the liquid-drop model at the angular momentum $\ell = 0$ [34] on ≈ 1 MeV as a rule, see Table I. The value of the liquid-drop contribution to the ^{210}Po fission barrier obtained in the new liquid-drop model with the deformation-dependent congruence (Wigner) energy term [40] is slightly smaller 10 MeV, which is close to the value $B_{\text{ld}}^{\text{S}} = 10.79$ MeV found in Ref. [34]. The values of the liquid-drop barrier of the ^{210}Po evaluated in the framework of eight different approaches belong to the range ≈ 10.5 to ≈ 12.5 MeV [41]. The value $B_{\text{ld}} = 11.83$ MeV obtained by fitting the ratio $R(E)$ is located in this range.

The absolute values of the ground-state $E_{\text{sp}}^{\text{gs}}$ and saddle-point $E_{\text{sp}}^{\text{saddle}}$ shell corrections obey the inequalities $|E_{\text{sp}}^{\text{gs}}| \gg |E_{\text{sp}}^{\text{saddle}}|$ [3,42]. The value of the pairing force correction is much smaller the shell correction related to the nonuni-

form distribution of the single-particle levels. Due to this, the value of shell-correction contribution to the fission barrier is $B_{\text{shell}}(0) \approx B_{\text{sp}}(0) = E_{\text{sp}}^{\text{saddle}} - E_{\text{sp}}^{\text{gs}} \approx -E_{\text{sp}}^{\text{gs}}$. Therefore, the values of $B_{\text{shell}}(0)$ for various nuclei should be close to the values of the ground-state shell correction $-E_{\text{shell}}^{\text{MNMS}}$ obtained in the macroscopic-microscopic finite-range liquid-drop model [35]. The absolute difference between $B_{\text{shell}}(0)$ and $-E_{\text{shell}}^{\text{MNMS}}$ for nuclei in Table I is smaller than 1 MeV, as a rule. This is supporting the reliability of obtaining values of both the fitted parameters and the fission barriers.

The values of γ_D^{-1} obtained by $R(E)$ fitting belong to the range $10 \text{ MeV} \leq \gamma_D^{-1} \leq 30 \text{ MeV}$, which is discussed in Ref. [21]. The values of γ_D^{-1} depend on the numbers of protons and neutrons [21]. The values of γ_D^{-1} presented in Table I also depend on the nucleonic composition of the nuclei. Unfortunately, the values of γ_D^{-1} for our set nuclei have not been theoretically studied.

So, the values of fitted parameters B_{ld} , $B_{\text{sp}}(0)$, and γ_D^{-1} obtained in our calculations for the description of the ratio $R(E)$ for the considered set of nuclei have reasonable values.

IV. CONCLUSIONS

The experimental values of the ratio $\Gamma_f(E)/\Gamma_n(E)$ are well described for the nuclei $^{180,181,182,184}\text{W}$, ^{185}Re , $^{186,187,188,190}\text{Os}$, $^{189,191}\text{Ir}$, $^{192,193,194,196}\text{Pt}$, $^{197,195}\text{Au}$, $^{196,198,199,200}\text{Hg}$, ^{201}Tl , $^{207,209}\text{Bi}$, $^{208,210,211,212}\text{Po}$, and ^{213}At in the framework of our statistical approach. Using the experimental values of the ratio $\Gamma_f(E)/\Gamma_n(E)$ we obtain the values of the fission barrier heights for 29 nuclei. The values of the statistical model parameters for the energy-level density used in our analysis are taken from Refs. [26,31] without any modification. The values of parameters B_{ld} , $B_{\text{sp}}(0)$, and γ_D^{-1} obtained by fitting the ratio $\Gamma_f(E)/\Gamma_n(E)$ in our approach are reasonable. The calculated values of the fission barrier heights are well agreed with the available experimental data and the theoretical values calculated in the macroscopic-microscopic finite-range liquid-drop model [38].

[1] R. Vandenbosch and J. R. Huizenga, *Nuclear Fission* (Academic Press, New York, 1973).
 [2] A. V. Ignatyuk *et al.*, *Yad. Fiz.* **21**, 1185 (1975) [*Sov. J. Nucl. Phys.* **21**, 612 (1975)].
 [3] A. V. Ignatyuk *et al.*, *Fiz. Elem. Chastits At. Yadra* **16**, 709 (1985) [*Sov. J. Part. Nucl.* **16**, 307 (1985)].
 [4] J. O. Newton, *Fiz. Elem. Chastits At. Yadra* **21**, 821 (1990) [*Sov. J. Part. Nucl.* **21**, 349 (1990)].
 [5] A. S. Iljinov *et al.*, *Nucl. Phys. A* **543**, 517 (1992).
 [6] V. Yu. Denisov and V. A. Plujko, *Problems of Physics of Atomic Nucleus Nuclear Reactions* (Publishing Polygraphic Centre "The University of Kiev," Kiev, 2013) [in Russian].
 [7] V. Yu. Denisov and I. Yu. Sedykh, *Eur. Phys. J. A* **54**, 231 (2018).
 [8] K. Jing, Ph.D. thesis, University of California, Berkeley, 1999, (unpublished).

[9] K. Mahata, *Pramana* **85**, 281 (2015).
 [10] V. Yu. Denisov and S. Hofmann, *Phys. Rev. C* **61**, 034606 (2000).
 [11] V. Yu. Denisov and I. Yu. Sedykh, *Chin. Phys. C* **45**, 044106 (2021).
 [12] N. Bohr and J. A. Wheeler, *Phys. Rev.* **56**, 426 (1939).
 [13] H. Eslamizadeh, *J. Phys. G* **44**, 025102 (2017).
 [14] V. Yu. Denisov and I. Yu. Sedykh, *Phys. Rev. C* **98**, 024601 (2018).
 [15] G. D. Adeev and P. A. Cherdantsev, *Yad. Fiz.* **18**, 741 (1973) [*Sov. J. Nucl. Phys.* **18**, 381 (1973)].
 [16] M. Brack and Ph. Quentin, *Phys. Scripta* **10A**, 163 (1974).
 [17] M. Diebel, K. Albrecht, and R. W. Hasse, *Nucl. Phys. A* **355**, 66 (1981).
 [18] M. Pi, X. Vinnas, and M. Barranco, *Phys. Rev. C* **26**, 733 (1982).

- [19] Z. Lojewski, V. V. Pashkevich, and S. Cwiok, *Nucl. Phys. A* **436**, 499 (1985).
- [20] M. Brack, C. Guet, and H.-B. Hakansson, *Phys. Rep.* **123**, 275 (1985).
- [21] J. A. Sheikh, W. Nazarewicz, and J. C. Pei, *Phys. Rev. C* **80**, 011302(R) (2009).
- [22] J. C. Pei, W. Nazarewicz, J. A. Sheikh, and A. K. Kerman, *Phys. Rev. Lett.* **102**, 192501 (2009); J. C. Pei *et al.*, *Nucl. Phys. A* **834**, 381c (2010).
- [23] C. Guet, E. Strumberger, and M. Brack, *Phys. Lett. B* **205**, 427 (1988).
- [24] J. O. Newton, D. G. Popescu, and J. R. Leigh, *Phys. Rev. C* **42**, 1772 (1990).
- [25] W. Dilg *et al.*, *Nucl. Phys. A* **217**, 269 (1973).
- [26] R. Capote *et al.*, *Nucl. Data Sheets* **110**, 3107 (2009).
- [27] A. V. Ignatyuk, G. N. Smirenkin, and A. S. Tishin, *Yad. Fiz.* **21**, 485 (1975) [*Sov. J. Nucl. Phys.* **21**, 255 (1975)].
- [28] V. M. Strutinsky, *Yad. Fiz.* **3**, 614 (1966) [*Sov. J. Nucl. Phys.* **3**, 449 (1966)]; *Nucl. Phys. A* **95**, 420 (1967); **122**, 1 (1968).
- [29] M. Brack *et al.*, *Rev. Mod. Phys.* **44**, 320 (1972).
- [30] W. J. Swiatecki, *Aust. J. Phys.* **36**, 641 (1993).
- [31] A. Mengoni and Y. Nakajima, *J. Nucl. Sci. Technol. (Abingdon, U. K.)* **31**, 151 (1994).
- [32] A. L. Goodman, *Nucl. Phys. A* **352**, 30 (1981).
- [33] T. Dossing and S. Aberg, in *Fifty Years of Nuclear BCS*, edited by R. A. Broglia and V. G. Zelevinsky (World Scientific, Singapore, 2013), p. 309.
- [34] A. Sierk, *Phys. Rev. C* **33**, 2039 (1986).
- [35] P. Moller *et al.*, *At. Data Nucl. Data Tables* **109-110**, 1 (2016).
- [36] M. Dahlinger, D. Vermeulen, and K.-H. Schmidt, *Nucl. Phys. A* **376**, 94 (1982).
- [37] G. N. Smirenkin, IAEA-Report INDC(CCP)-359 (1993) (see also <https://www-nds.iaea.org/RIPL-3/>).
- [38] P. Moller, A. J. Sierk, T. Ichikawa, A. Iwamoto, and M. Mumpower, *Phys. Rev. C* **91**, 024310 (2015).
- [39] M. Wang *et al.*, *Chin. Phys. C* **41**, 030003 (2017).
- [40] K. Pomorski, *Phys. Scr.* **T154**, 014023 (2013); K. Pomorski and F. Ivanyuk, *Int. J. Mod. Phys. E* **18**, 900 (2009).
- [41] R. N. Sagaidak and A. N. Andreyev, *Phys. Rev. C* **79**, 054613 (2009).
- [42] Z. Patyk and A. Sobiczewski, *Nucl. Phys. A* **491**, 267 (1989).